Materials Science & Engineering A 590 (2014) 97–100

Contents lists available at ScienceDirect

Materials Science & Engineering A

journal homepage: www.elsevier.com/locate/msea

Rapid communication

Dynamic properties evaluation of 2519A aluminum alloy processed by interrupted aging

Lingying Ye*, Gang Gu, Xinming Zhang, Daxiang Sun, Haichun Jiang, Pan Zhang

School of Materials Science and Engineering, Central South University, Changsha 410083, China

ARTICLE INFO

Article history:
Received 3 August 2013
Received in revised form
22 September 2013
Accepted 9 October 2013
Available online 19 October 2013

Keywords:
Microstructure
2519A aluminum alloy
Dynamic property
Interrupted aging

ABSTRACT

Dynamic properties of 2519A aluminum alloy processed by interrupted aging are assessed in this work. At strain rate of 6900 s^{-1}, the dynamic yield strength and absorption energy of this material are up to 690.9 MPa and 335.5 MJ/m^3, respectively. Denser and finer θ′ precipitates contribute to these enhancements.

1. Introduction

Lightweight aluminum alloys with high strength have been widely used as armor for combat vehicles. Alloys 5083 and 7039 were developed for this application in early days [1]. Although both alloys 5083 and 7039 have high strength in the aluminum alloy family, an alloy with higher strength and similar density is always desirable to improve the performance of armored vehicles. In need of higher strength materials, 2519A was developed and has been shown to exhibit superior mechanical and ballistic property characteristics for lightweight combat vehicle applications.

2519A was used at T87 temper (solution, cold rolling, and then artificial aging) with a proper combination of mechanical properties, ballistic resistance and resistance to stress corrosion cracking during these years [2–4]. Zhang et al. [5] investigated the dynamic behavior of 2519A-T87 alloy with strain rates ranging from 600 to 7000 s^{-1}. The dynamic yield strength of it could reach 530 MPa at a strain rate of 5800 s^{-1}.

Interrupted aging is a new way to improve the properties of aluminum alloys [6,7]. 2519A alloy processed by interrupted aging (solution, pre-aging, cold rolling, then interrupted aging, re-aging) was named 2519A-T9I6 alloy in this work [8,9]. The yield strength, tensile strength and elongation rate of 2519A-T9I6 alloy were 501 MPa, 540 MPa and 14.3% [9], respectively, compared to 431 MPa, 470 MPa and 9.7% of 2519A-T87 alloy. In the present study, the dynamic responses of 2519A aluminum alloy are investigated for two different heat treatment conditions, T87 and T9I6. Because T9I6 process is a new thermomechanical processing technique for 2519A, its dynamic properties have to be accessed to compare with T87. It is also essential to clarify the structural evolution during deformation.

2. Experimental section

Dynamic impacting tests at strain rates of 1300 s^{-1}, 3300 s^{-1}, 5300 s^{-1} and 6900 s^{-1} were carried out at 293 K on a split Hopkinson pressure bar (SHPB) setup. The cylindrical specimens with the sizes of 4 mm in thickness and 6 mm in diameter were made for the testing. Microstructure characterizations of all impacted specimens were observed by a transmission electron microscope (TEM, Tecnai $G^2$20) operating at 200 kV. The disk specimens for TEM were cut out from cross section of the impacted specimens, polished mechanically to the range 0.05–0.07 mm. Then electro-polished in a 70% ethanol and 30% nitric acid solution at 248 K by a twin-jet equipment operated at 20 V. Volume fractions of the precipitates were calculated by Image J. The calculation for a type of alloy was based on at least 3 TEM bright-field images which were obtained from different areas of a sample.

3. Results

The true stress–strain curves at different strain rates (1300 s^{-1}, 3300 s^{-1}, 5300 s^{-1} and 6900 s^{-1}) of the studied alloys are shown

* Corresponding author. Tel./fax: +86 731 88830265.
E-mail address: lingyingye@csu.edu.cn (L. Ye).

0921-5093/$ - see front matter © 2013 Elsevier B.V. All rights reserved.
http://dx.doi.org/10.1016/j.msea.2013.10.016

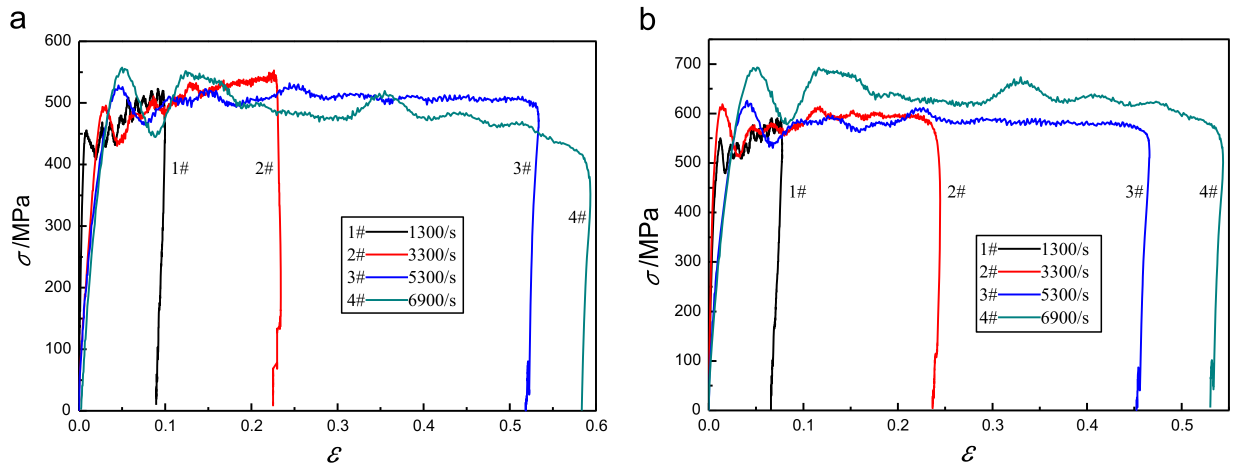

Fig. 1. True stress–strain curves of 2519A alloy with T87 (a) and T9I6 (b) temper at different strain rates.

in Fig. 1. 2519A-T9I6 alloy, benefiting from its high yield strength at quasi-static tensile test, has a higher dynamic yield strength than T87 temper at all strain rates. At strain rate of 6900 s^{-1}, the dynamic yield strength of 2519A-T9I6 alloy is up to 690.9 MPa, compared with 554.9 MPa of 2519A-T87. As for dynamic mechanical properties, T9I6 process has an advantage over T87 process. The stress–strain curves of 2519A-T9I6 alloy indicate that it has a higher flow stress than that of 2519A-T87 alloy at all strain rates. The high yield strength of 2519A with T9I6 temper at quasi-static tensile test contributed to its high dynamic yield strength. Otherwise, its high yield strength would result in a smaller strain than 2519A-T87 alloy at a same strain rate.

TEM bright-field images and corresponding SAD patterns of the studied alloy with different tempers impacted at different strain rates are shown in Fig. 2. Before impact tests, the alloy plate contains θ′ precipitate mainly in 2519A alloy with the two different tempers (Fig. 2(a) and (b)). Also, the orientation relationships between the θ′ precipitates and the Al-matrix are kept with $(0\,0\,1)_{\theta'} \| (0\,0\,1)_{Al}$ and $[1\,1\,0]_{\theta'} \| [1\,1\,0]_{Al}$ on the $\{1\,0\,0\}_{Al}$ habit plane. It is obvious that the precipitates in 2519A-T9I6 alloy are finer and more densely distributed than that in 2519A-T87 alloy and this feature has been kept at all strain rates. Fig. 2(c) and (d) indicates that the precipitates of the alloys at both tempers barely changed at the strain rate of 1300 s^{-1}. As the strain rate reached 3300 s^{-1} or higher, however, the precipitates in 2519A-T87 alloy barely coarsened. Because the deformation energy resulted from severe plastic deformations, most of precipitates in 2519A-T87 alloy began to decompose and dissolve in the α-Al phase (see Fig. 2(e) and (g)). Meanwhile, Fig. 2(f) shows, in 2519A-T9I6 alloy, that the θ′ precipitate orientation relationships with Al matrix still hold true, and the thickening effect of θ′ plates is observed. At strain rate of 5300 s^{-1}, only a few precipitates could be found in 2519A-T87 alloy and the volume fraction of the remaining precipitates is 10.4%, compared to 17.9% of 2519A-T9I6 alloy. It could be concluded that the precipitates in 2519A-T9I6 alloy gained better stability during severe plastic deformation and presented a weaker tendency to coarsen and transform to θ phase or dissolve.

4. Discussion

When compared to tests conducted in static or quasi-static conditions, the impacted behaviors of materials are different. The ultimate or yield strength will increase and the elongation will decrease during the process of a high strain rate test. The wavy stress–strain curves appearance is owing to the effect of stress strain strengthening and thermo-softening which are shown in Fig. 1. The amount of dislocations may multiply rapidly due to the short deformation time in the high speed impact process. The dynamic recovery may not happen and the sub-grains may not form either. As a result, the density of the dislocation in grains will keep at a high level and the storing energy will reach the driving power of DRX, and all these will lead to the DRX finally.

It also could be found in Fig. 1 that a higher strain rate would lead to a higher stress–strain curve because of strain hardening. This could be explained by strain rate sensitivity (SRS). The effect of strain rate on the flow stress can be expressed by the SRS parameter *m*, which is defined as [10]

$$m = \frac{d \log \sigma}{d \log \varepsilon} \tag{1}$$

where σ and ε are the stress and the strain rate of impact tests, respectively. The SRS is affected by many factors: the grain size, the dislocation, the temperature, the processing route, etc. Shown in Fig. 3, the results of the calculated *m* values of studied alloys are indicated. Fig. 3 also demonstrates that the SRS parameter of 2519A alloy with T9I6 temper is higher than that of 2519A-T87 alloy. In other words, 2519A-T9I6 alloy would have better strain strengthening effects as the strain rate increases. As a kind of armor, the self-strengthening resulted from strain strengthening could protect the material from failure during dynamic damage processes.

2519A aluminum alloy is a typical age-hardenable alloy which is strengthened by the semicoherent fine θ′ precipitate. It has been indicated that the precipitation reaction below 523 K proceeds through a well accepted sequence of transformations [11]: Al_{ss} (supersaturated)→GP zones→θ″(or GP II zones)→θ′→θ. The thermal evolution of metastable θ′ phase is dramatic with increasing temperature. Fig. 2 reveals a microstuctural evolution of the precipitates in 2519A-T87 and 2519A-T9I6. The temperature change resulted from energy absorption is considered to be the main factor affecting the phase transformation in 2519A alloy. The absorption energy per unit volume for a sample, up to a strain ε_e, can be evaluated by integrating the area under the stress–strain curve, namely [12]

$$W = \int_0^{\varepsilon_e} \sigma \mathrm{d}\varepsilon \tag{2}$$

where *W* is the absorption energy per unit volume of specimen, ε_e is the maximum strain, and ε and σ are the true stress and true strain, respectively. Temperature change due to the absorption energy can be estimated from the following equation [13]:

$$\Delta T = \beta \rho^{-1} C_V^{-1} \int_0^{\varepsilon_e} \mathrm{d}\varepsilon \tag{3}$$